Heliyon 8 (2022) e08768

Contents lists available at ScienceDirect

Heliyon

journal homepage: www.cell.com/heliyon

Research article

Sliding Mode Observer Design for decentralized multi-phase flow estimation

Abolfazl Varvani Farahani [a,*], Soroush Abolfathi [b]

[a] Faculty of Engineering, Shahid Beheshti University, Tehran, Iran
[b] School of Engineering, University of Warwick, Coventry, UK

ARTICLE INFO

Keywords:
Sliding Mode Observer
Multi-phase flow measurement
Uncertainty quantification
Disturbance

ABSTRACT

Robust flow measurement in multi-phase systems has extensive applications in understanding, design, and operation of complex environmental, energy and industrial processes. The nonlinearity and spatiotemporal variability of the interactions between different flow phases makes the multi-phase flow measurement a challenging task. Two Sliding Mode Observer (SMO) schemes are proposed in this study for the state estimation of a decentralized multi-phase flow measurement system. The developed observers are shown to be theoretically valid and numerically applicable for a real-life case study data. The multi-phase flow system considered in this paper can be described as two interconnected sub-systems including fluid and gas sub-systems, and two scenarios are considered in the design of the observers. The first scenario considers the interconnections as bounded disturbance (SMOD), while the second scenario considers the interconnections as an uncertainty (SMOU). Hence, the Sliding Mode Observers are adopted to mitigate the effects of disturbance in the system and uncertainties in the parameters. Numerical simulations are conducted using MATLAB and dynamic HYSYS simultaneously, using the data obtained from field-based multi-phase flow measurements. The results demonstrate the appropriateness and robustness of the proposed Sliding Mode Observer (SMO) for estimation of the multi-phase fluid specifications including the density, velocity, and the volume phases fraction in each subsystem. The analysis of the results highlights that the proposed model is computationally efficient with fast transient response, accurate tracking capability of the real process data, and very low steady-state error. This study shows that choosing an appropriate Lyapunov-Krasovsky function results in the asymptotic stability of the decentralized system and improves the performance of the proposed observers. Uncertainty analysis is conducted on the velocity estimation results obtained from the Sliding Observers. Overall, SMOU method shown better performance with RMSE of 0.24%, while RMSE of 0.46% was achieved for the SMOD. Comparison of the numerical results with the field-based flow measurement, as a benchmark, shows that although uncertainty in SMOU is approximately half of the uncertainty in SMOD, state estimation for both schemes was achieved in a finite time with high order of precision. It was shown that both observers developed in this study are well capable of estimating the multi-phase flow variables and states.

1. Introduction

Multi-phase flows are common features in a broad range of environmental and industrial processes including wastewater treatment reactors, chemical processes, pharmaceuticals, biotechnology, oil and gas industry. Gas–liquid–solid and gas–liquid multi-phase flow systems have a variety of applications in utilities, production, process and pipeline transport [1]. Robust flow measurement is one of the most challenging tasks in dealing with multi-phase flow systems [2, 3, 4]. Detailed information on the volume and state of the flow is essential for optimal design and operation of multi-phase flow processes as well as reducing the potential damage to the equipment due to fluctuations in the state and parameters of the flow. In many industrial processes the multiphase flow emerges by line pressure drop and phase transfer phenomenon between liquid and gas phases, leading to formation of liquid-gas or oil-gas two-phase flow [5]. Given that accurate measurement of two-phase flows is not possible in most of the cases, estimation of two-phase liquid-gas flow systems (e.g., water-steam flows) is vital

* Corresponding author.
E-mail addresses: A_Varvani@sbu.ac.ir (A. Varvani Farahani), Soroush.Abolfathi@Warwick.ac.uk (S. Abolfathi).

https://doi.org/10.1016/j.heliyon.2022.e08768
Received 22 March 2021; Received in revised form 18 September 2021; Accepted 11 January 2022

for process controlling, optimal energy consumption and prevention of incidents [6]. Flow measurement in multi-phase flow systems plays a key role in controlling the process conditions and determining the volume fraction of each flow phase.

Despite major technological advancement in precise single-phase flow measurement techniques, to this date, the existing multi-phase flow measurement techniques (i.e. liquid, gas and solid) are not very accurate [7]. The conventional multi-phase flow measurement techniques are either costly and relying in the use of sophisticated equipment or are not capable of making thoroughgoing direct measurements due to technological limitations. Adoption of the soft sensors is an alternative approach to overcome the technological problems and limitations associated with the existing multi-phase flow measurement techniques and enhance the accuracy of flow measurement in complex multi-phase flow systems [8].

Previous studies have reviewed and assessed different multi-phase flow measurement methodologies including phase separation, inferential approach, microwave attenuation, gamma attenuation, Impedance and cross-correlation method for estimating the flow characteristics, i.e. phase fraction and velocity of multiphase flow in pipeline [9]. Goes et al. [10] proposed a mass flowrate measurement system for liquid-gas two-phase flow measurement, consisting of an orifice plate or Venturi flow meter coupled with a non-intrusive impedance void fraction system. Gysling and Meters [11], developed a pulsed-array sonar flow meter with a compositional model soft sensor to facilitate the use of flow composition data. Shia et al. [12] proposed one-sided Doppler mode ultrasonic transducer with continuous wave, coupled with a conductance sensor to obtain the holdup in pipe and Doppler shift signal in the medium.

The literature shows that the use of non-intrusive techniques for estimation of multiphase flow characteristics has rapidly found favor in the recent years. Sarkodie et al. [13] described the existing limitations and future research needs for non-intrusive optical infrared sensors for liquid-gas multiphase flow characterization in pipeline. Baba et al. [14] investigated the effects of high-order viscosity on the main characteristics of two-phase flows such as pressure gradient, slug production frequency, and liquid holdup, with heavy mixture of oil and gas using an advanced non-intrusive Electrical Capacitance Tomography method. Despite these techniques have been extensively used for measuring two-phase gas-solid mixture flow, the particle distribution adversely affects the nonlinear response of the measurement and consequently reduce the accuracy of the flow measurements [15]. A reliable measurement of multi-phase flow characteristics (e.g., flow rate, phase velocity, and phase fractions) can be influenced by several parameters including the flow pattern, phase properties, flow condition, flow region, multi-phase flow system characteristics and the associated boundary conditions, environmental conditions, instrumentation, and measurement technology [16].

Unscented Kalman Filter (UKF) and Ensemble Kalman Filter (EnKF) have been adopted to improve the forecast in the flow estimation of a lowland conceptual hydrologic model [17]. The UKF and EnKF filters widely used in steam-water processes, for example, ensemble Kalman filter square root (EnKF-SR) has been adopted to estimate steam temperature and water level in steam-water two-phase flows [18]. In addition to the widespread use of soft sensors for approximating multi-phase flow quantities, this method can also be used in estimating the quality of the flow, i.e. steam quality, gas and liquid volume fraction, as a process variable [19]. Santos et al. [20] illustrated soft sensor combining the fast conductance sensors with appropriate computational algorithms is capable of rigorous measurement of two-phase flow states in pipeline. Yan et al. [21] conducted a comparative study to investigate performance of different soft sensors and computing methods for multi-phase fluid flow estimation with a particular focus on the measurement of individual phase fractions and velocities.

Sliding mode control (SMC) is a variable structure control method that can alters the dynamics of a nonlinear system by applying a discontinuous control signal that forces the system to 'slide' along a cross-section of the system's normal behavior. SMC can be used as a robust tool for the design of state observers with the capability of reducing estimator error dynamics to zero in finite time, as nonlinear high-gain observers. One of the most attractive features of a sliding mode observer is its capability to eliminate the effects of disturbances by using intermittent inputs which lead the estimation error trajectory to an absorbing sliding manifold in finite time [22]. The global terminal sliding is one of the suitable methods for fast transfer of system states to its equilibrium point and to ensure that the control signal is non-singular [23]. In complex multi-phase flow systems, due to the changing operational conditions and the presence of diverse disturbance sources, i.e. random fluctuation of input flow or consumption of equipment and noises in the transmitting signals, the flow parameters and the state of the system is subjected to large uncertainties. Hence, monitoring and measurements in complex nonlinear multi-phase systems using conventional methods, such as state feedback and linear control, cannot provide a robust and reliable flow estimation performance. To compensate the uncertainties and mitigate the disturbances, advanced control methods such as Adaptive, Robust and Sliding mode have been successfully tested [24, 25, 26, 27, 28, 29]. Sliding Mode control method has the advantage of providing superior performance for those multi-phase flow systems with strong perturbation and spatiotemporal changes in the control parameters [29]. Nikoofard et al. [30] developed a Robust-Adaptive observer to estimate the state of two-phase flow of oil and gas from a reservoir during the drilling operation. Robust adaptive observers using a prediction model have been proposed for high-order complex systems that are exposed to unmeasurable disturbances and large fluctuations in the multi-phase flow characteristics [31, 32].

The complexity of multi-phase flow measurements in a wide variety of industries (e.g., oil and gas, process engineering, environmental monitoring) highlighted the need for an improved reliability and safety in the flow measurement. Therefore, number of studies investigated monitoring of the system states, fault detection, isolation, and restoration by adopting the Sliding Mode control method [27, 28, 29, 30]. To tackle large uncertainties associated with the multi-phase flow state and environmentally varying conditions, Robust and Sliding Mode control methodologies have been widely investigated and successfully implemented for a range of applications [33, 34, 35, 36]. Liu et al. [39] developed a Robust Observer for a stochastic neutralized system with uncertainty using Sliding Mode method with a guaranteed finite time limit to achieve an appropriate sliding surface.

Multi-phase flows in many environmental and industrial processes are subject to nonlinear and complex changes in the flow regime, composition of different phases, temperature and pressure fluctuations [40], [41], [42], [43], [44]. These nonlinearities in multi-phase flow systems are further intensified due to the existence of disturbance sources, the effects of environmental conditions, and specifications of the multi-phase flow system. However, with understanding the underlying physical processes governing the multi-phase flow behavior, it is possible to have a reliable estimation of the minimum and maximum of all the factors that influence the nonlinear behavior and fluctuations in the system, which can further improve accuracy of the results obtained from the Sliding Mode technique.

This study aims to design Sliding Mode Observer (SMO) for distributed multi-phase flow system in the presence of disturbance and uncertainty. A nonlinear system subject to the time-varying uncertainty with bounded norm is adopted in this study to deal with the synthesis of the proposed observer. Hence, SMO is developed for multi-phase flow measurement to eliminate the effects of disturbances and overcome the uncertainties triggered by the fluctuations in the flow parameters. To provide a comprehensive analysis of the performance of the proposed SMO model, two scenarios are defined. The first scenario adopts Sliding Mode Observer with disturbance (SMOD), where the interconnections between two subsystems are considered as a disturbance. The second

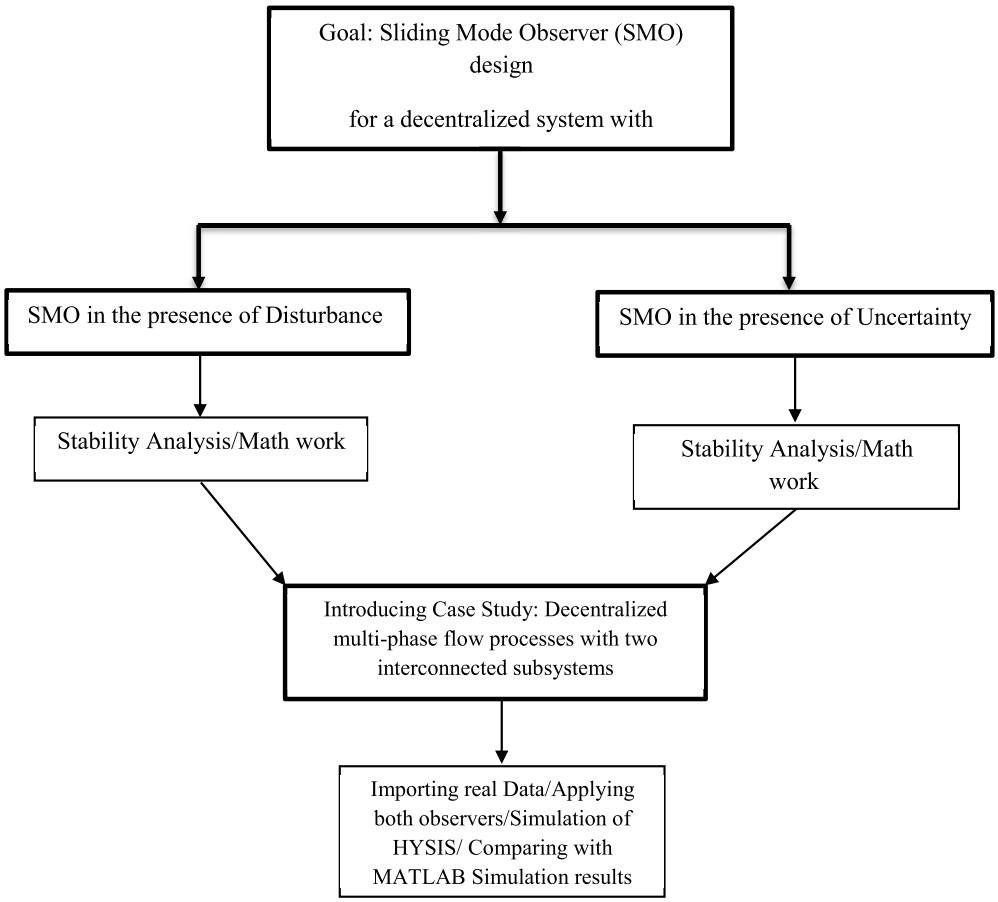

Fig. 1. Detailed block diagram of the proposed SMO approach.

scenario adopts Sliding Mode Observer with uncertainty (SMOU) and investigates the variations in multi-phase flow parameters and states caused by the uncertainties due to the changes in interconnections between the subsystems.

This paper is organized as follows: The structure of the sliding mode observer for the two SMOD and SMOU scenarios is developed, and proof of the observer's convergence is demonstrated in §2. Given that the distributed multi-phase flow model is quite similar to the stated dynamic model, a case study of multi-phase flow system is considered and the proposed observers are implemented for the case study data in §3. Section 4 describes and discusses the simulation results, and the concluding remarks are described in Section 5.

2. Sliding Mode Observer Design

The majority of the industrial systems involving multi-phase flow are usually composed of two interconnected subsystems to process each phase separately. These subsystems can be modeled as a class of non-linear interconnected system:

$$v_t^i(s,t) = -A_i v_s^i(s,t) + Q_i(s,t) + h_j(s,t), \quad i,j = G,\ L \& i \neq j \tag{1}$$

$$y_i = \int_0^L C v_i(s,t) ds \tag{2}$$

where A_i are states matrices of subsystems with appropriate dimensions, s denotes the Spatial position (m), t is time (sec), $v_i \in \mathbb{R}$, $y_i \in \mathbb{R}$, $Q_i \in \mathbb{R}$ and $h_j \in \mathbb{R}$ vectors denote the state, output, input (flux) and the interconnections of the two subsystems, respectively. It is assumed that $h_i(s,t)$ and $Q_i(s,t)$ are differentiable with respect to v. $h_j(s,t)$, as interconnection terms between the subsystems play an important role in the design of the decentralized system. This is due to the fact that although these interconnection terms may be measurable but their effects on the states of other subsystems are unknown. All states of the subsystems will be determined based on the dynamic models following the determination of these interconnections. Given that in soft sensors, usually the main state variables are unknown and unmeasurable, they will be determined though other measurable variables. In this study, the main states (gas and liquid velocity, and phase fractions) are not directly measurable, and therefore they are estimated by other measurable variables (e.g., pressure, temperature, and single-phase gas flow) and using dynamic simulation model for multi-phase flows.

SMO design for a non-linear interconnected system described by Eq. (1) and Eq. (2) is conducted and the performance of the developed SMO is tested using two scenarios. In the first scenario, the interconnection between the subsystems is considered as a disturbance vector (§2.1) while in the second scenario the interconnection between the subsystems is considered as an uncertainty in the flux (§2.2). A detailed block diagram of the proposed approach is presented in Fig. 1, to clarify the design procedure and the modeling structure.

2.1. Scenario 1 - SMOD

In the presence of a disturbance, observers must be designed to estimate the variables, and compensate for the disturbance term. Given that the overall system is considered as a combination of two interconnected systems, in the first scenario, the interconnections between two subsystems are considered as a disturbance and in addition to estimating the state variables, the observer is expected to eliminate the effects of perturbation. Therefore, the general form of the Eq. (1) can be rewritten as follows:

$$V_t(s,t) = -AV_s(s,t) + Q(s,t) + H(s,t) \tag{3}$$

where A, v, Q and H are the state matrix, variables, flux, and subsystems interconnections, respectively. The available measurements are acquired by pressure sensors, outlet single-phase flow meters and analyzers. By considering interconnection term $H(s,t)$ as a disturbance, the proposed observer is defined as [45]:

$$\hat{V}_t(s,t) = -A\hat{V}_s(s,t) + \hat{Q}(s,t) + L \cdot sign(\sigma) \tag{4}$$

where $\hat{V}(s,t)$ is the estimated states, $\hat{Q}(s,t)$ is the flux estimation, L is the observer gain, $sign(\sigma)$ denotes the signum function of σ and the sliding surface is defined as:

$$\sigma(s,t) = \tilde{v}(s,t) = V(s,t) - \hat{V}(s,t) \tag{5}$$

In the Sliding Mode technique, the state trajectory of the system is bounded in a chosen manifold by an appropriate control action. This manifold is termed as switching surface or a sliding surface. Sliding surface is used to improve the controller/observer performance by minimizing or eliminating the time to reach the sliding phase [46].

$\sigma = V(s,t) - \hat{V}(s,t)$ is the estimation error and as $\tilde{V}(0,t) = V(0,t) - \hat{V}(0,t)$, thus to have estimation error dynamic, the time derivative of $\sigma(s.t)$ is given by Eq. (6):

$$\dot{\sigma} = \dot{V}(s,t) - \dot{\hat{V}}(s,t) = \underbrace{-A(s,t)\frac{\partial V}{\partial s}(s,t) + Q(s,t)}_{\dot{V}(s,t)} + \underbrace{A(s,t)\frac{\partial \hat{V}}{\partial s}(s,t) - \hat{Q}(s,t)}_{\dot{\hat{V}}(s,t)} - \underbrace{H(s,t)}_{\text{interconnection}} - \underbrace{Lsign(\sigma)}_{\text{observer gain}} \tag{6}$$

Then, as $t \to \infty$, state of the observer converges to state of the system, and therefore, $\tilde{V}(0,t) = V(0,t) - \hat{V}(0,t) \to 0$. In order to find the minimum observer gain to ensure observer stability, this study adopts the Lyapunov approach to sliding mode observer as follows [47]:

$$V = \frac{1}{2}\sigma^2 \geq 0 \tag{7}$$

In order to ensure and prove the stability of the sliding mode observer, the following inequality must be satisfied [47]:

$$\dot{V} = \sigma\dot{\sigma} \leq -\eta\sigma^2 \tag{8}$$

where η is a positive constant. The estimation error on $A\frac{\partial V}{\partial s}$ is considered to be bounded by some known function γ, so that:

$$A(t,s)\frac{\partial V}{\partial s}(t,s) + Q(t,s) - \hat{Q}(t,s) - A(t,s)\frac{\partial \hat{V}}{\partial s}(t.s) \leq \gamma \tag{9}$$

The sliding condition is assumed as follows:

$$\begin{aligned} \dot{V} &= \sigma\dot{\sigma} = \sigma\dot{\tilde{v}} \\ &= \sigma(\gamma - H - L) \\ &< \sigma(\gamma - L) \end{aligned} \tag{10}$$

According to the inequality presented in Eq. (8), the following can be obtained:

$$\begin{aligned} &\sigma\dot{\sigma} \leq -\eta\sigma^2 \\ &\sigma\dot{\sigma} \leq \sigma(\gamma - L) \leq -\eta\sigma^2 \\ &\frac{\gamma}{\sigma} + \eta \leq L \end{aligned} \tag{11}$$

Then $L_{\min}$ can be derived as:

$$L\frac{\gamma}{\sigma}_{\min} \tag{12}$$

Hence, to reduce the chattering, observer gain can be considered as $L = L\frac{\sigma}{|\sigma|+\delta}_{\min}$, where δ, which is known as tuning parameter, is a small positive scalar ranging between 0 to 1. From Eq. (12) it can be observed that as $\delta \to 0$, function L tends to be a signum function of L [47].

2.2. Scenario 2 - SMOU

Although flow measurement in multiphase systems is always associated with some level of uncertainty based on the flow measurement technology, the variations in the process conditions, and flow variables impose additional uncertainties on the system. This additionally imposed uncertainties due to the multi-phase flow variables should be explicitly specified in the observer design approach. In scenario 2, the variations in multi-phase flow parameters (i.e. density, viscosity and wall friction factor), and states (i.e. phases velocities, pressures and phase volume fractions) which cause changes in the interconnections between subsystems, are considered as an uncertainty. Thus, considering Eq. (3), the final form of the system's equations in the presence of uncertainty are derived as follows:

$$\begin{aligned} &\frac{\partial v_i}{\partial t} = -(A_i + \Delta A_i)\frac{\partial v_i}{\partial s} + \tilde{Q}_i, \quad i \neq j = G.L \\ &y_i = Cv_i \end{aligned} \tag{13}$$

where $C = [I_p 0_{p\times(n-p)}]$ and C^T is the transpose of C so that $CC^T = I$ will be held, v_i denotes states, y_i is the outputs of each subsystem, and ΔA_i denotes the fluctuations of the system state due to the changes in the interconnections between the subsystems and it will apply to the following hypothesis:

Hypothesis 1. Assuming that the uncertainties are bounded norms:

$$\Delta A_i = M_i^a H_a N_i^a \tag{14}$$

where $H_a \in R^{k\times l}$ and $F_a^T F_a < I_{l\times l}$ so that F_a determines the uncertainty structures and parameter's fluctuations.

$$M_i^a = \begin{bmatrix} 0 & 0 & \rho_l \\ 1-\alpha_l & 0 & \rho_g \\ (-\alpha_l)u_g & \rho_l(\frac{1}{C_0} - 1) & u_g(\rho_l - \rho_g) \end{bmatrix}^{-1} \tag{15}$$

$$H_i^a = \begin{bmatrix} 0 \\ h_i \\ 0 \end{bmatrix}, \quad N_i^a = [111] \tag{16}$$

2.2.1. SMOU design

This study adopts the methodology outlined by Galvan et al. [37] to design the observer structure, with the extended form defined as follows:

$$\begin{aligned} &\frac{\partial \hat{v}_i}{\partial t} = -A_i\frac{\partial \hat{v}_i}{\partial s} + \hat{Q}_i + L_i(y - \hat{y}) + \alpha_i, \quad i \neq j = G, L \\ &\hat{y}_i = C\hat{v}_i \end{aligned} \tag{17}$$

where $\hat{v} \in R^n$ is the vector of the state's estimation, α_i is the sliding mode gain for the ΔA_i uncertainty compensation and $L_i \in R^{n\times p}$ is the observer gain, which are determined using the LMI solution presented in Eq. (18):

$$(A_i - L_iC)^T P + P(A_i - L_iC) < 0, \quad \text{for } i = 1, \ldots, M \tag{18}$$

Lemma 1. *For any pair of X and Y matrices with appropriate dimensions, there is a β that the following inequality holds [48]:*

$$X^TY + Y^TX \leq \beta X^TX + \beta^{-1}Y^TY, \quad \beta > 0 \tag{19}$$

Lemma 2. *For a symmetric matrix M which is partitioned into blocks as follows [49]:*

$$M = \begin{bmatrix} Z & S \\ S^T & R \end{bmatrix} \tag{20}$$

where Z and $R > 0$ are symmetric and square matrices, the following characteristics are equivalent:

$$M > 0,$$
$$Z - SR^{-1}S^T > 0 \tag{21}$$

Theorem 1. *The estimation error between the systems described by Eq. (4) and Eq. (17) asymptotically converges to zero, if there exist a positive definite matrix $P \in R^{n\times n}$, matrices $W_i \in R^{n\times p}$ and scalar $\varepsilon > 0$, such that for $i = 1, \ldots, M$ we have:*

$$\begin{bmatrix} A_i^T P + PA_i - C^T W_i^T + W_i C + 2\varepsilon^{-1} N_i^{aT} N_i^a & PM_i^a \\ M_i^{aT} P & -\varepsilon^{-1} I \end{bmatrix} < 0 \tag{22}$$

where C, C^T, M_i^a and N_i^a are known matrices [from Eq. (3), Eq. (15) & Eq. (16)] and the following conditions are held:

$$\begin{cases} \text{If } r \neq 0, \text{ then } \alpha_i = \varepsilon^{-1}\hat{v}^T N_i^{aT} N_i^a \hat{v} P^{-1} C^T \frac{s}{\|s\|^2} \\ \text{If } r = 0, \text{ then } \alpha_i = 0 \end{cases} \tag{23}$$

where s is the sliding surface, The observer's gains are computed by $L_i = P^{-1}W_i$.

Proof. To prove the above-mentioned Theorem 1, Lemma 1 and 2 are adopted as follows:

In order to prove the stability of the proposed observer, the output and state errors are defined as follows:

$$\begin{cases} r = y - \hat{y} \\ e = v - \hat{v} \end{cases} \tag{24}$$

Thus, the dynamics of estimation error is:

$$\dot{e} = \dot{v} - \dot{\hat{v}} \tag{25}$$
$$\dot{e} = \sum_{i=1}^{M} ((A_i - L_i C)e + \Delta A_i v - \alpha_i) \tag{26}$$

and therefore, the sliding surface will be defined as:

$$s = r = Ce = C(v - \hat{v}) \tag{27}$$

Now, the following Lyapunov function is considered:

$$V = s^T Q s \tag{28}$$

where Q is appropriate symmetric matric so that $rank(Q) = p$. Using Eq. (25) and Eq. (26), time derivative of Lyapunov function is derived as:

$$\begin{aligned} \dot{V} &= \dot{s}^T Q s + s Q \dot{s} \\ \dot{V} &= \sum_{i=1}^{M} (e^T (A_i - L_i C)^T C^T Q C e + v^T \Delta A_i^T C^T Q C e \\ &\quad - \alpha_i^T C^T Q C e + e^T C^T Q C (A_i - L_i C) e + e^T C^T Q C \Delta A_i v - e^T C^T Q C \alpha_i \end{aligned} \tag{29}$$

With the assumption of $P = C^T Q C$, Eq. (29) can be written as:

$$\dot{V} = \sum_{i=1}^{M} (e^T ((A_i - L_i C)^T P + P(A_i - L_i C))e + v^T \Delta A_i^T P e + e^T P \Delta A_i v - 2e^T P \alpha_i \tag{30}$$

Applying Lemma 1 and 2, the following can be derived:

$$\begin{aligned} v^T \Delta A_i^T P e + e^T P \Delta A_i v &= v^T (M_i^a \mathrm{H}_a N_i^a)^T P e + e^T P M_i^a H_a N_i^a v \\ &= e^T P M_i^a H_a N_i^a v + v^T N_i^{aT} H_a^T M_i^{aT} P e \\ &< \varepsilon e^T P M_i^a M_i^{aT} P e + \varepsilon^{-1} v^T N_i^{aT} N_i^a v \end{aligned} \tag{31}$$

Therefore, time derivative of Lyapunov function can be estimated as follows:

$$\begin{aligned} \dot{V} = \sum_{i=1}^{M} &(e^T ((A_i - L_i C)^T P + P(A_i - L_i C) + \varepsilon e^T P M_i^a M_i^{aT} P)e \\ &+ \varepsilon^{-1} v^T N_i^{aT} N_i^a v - 2e^T P \alpha_i \end{aligned} \tag{32}$$

Replacing the state expression, $v = \hat{v} + e$, the following equality can be obtained:

$$\begin{aligned} \varepsilon^{-1} v^T N_i^{aT} N_i^a v &= \varepsilon^{-1} (\hat{v} + e)^T N_i^{aT} N_i^a (\hat{v} + e) \\ &= \varepsilon^{-1} \hat{v}^T N_i^{aT} N_i^a \hat{v} + \varepsilon^{-1} \hat{v}^T N_i^{aT} N_i^a e + \varepsilon^{-1} e^T N_i^{aT} N_i^a \hat{v} \\ &\quad + \varepsilon^{-1} e^T N_i^{aT} N_i^a e \end{aligned} \tag{33}$$

Now, by adopting $\beta = 1$ and using Lemma 1, Eq. (33) can be derived as follows:

$$\begin{aligned} &\varepsilon^{-1} \hat{v}^T N_i^{aT} N_i^a \hat{v} + \varepsilon^{-1} \hat{v}^T N_i^{aT} N_i^a e + \varepsilon^{-1} e^T N_i^{aT} N_i^a \hat{v} + \varepsilon^{-1} e^T N_i^{aT} N_i^a e \\ &\quad \leq 2\varepsilon^{-1} \hat{v}^T N_i^{aT} N_i^a \hat{v} + 2\varepsilon^{-1} e^T N_i^{aT} N_i^a e \end{aligned} \tag{34}$$

and therefore, the new inequality can be written as Eq. (35):

$$\begin{aligned} \dot{V} \leq \sum_{i=1}^{M} &(e^T ((A_i - L_i C)^T P + P(A_i - L_i C) \\ &+ \varepsilon e^T P M_i^a M_i^{aT} P + 2\varepsilon^{-1} N_i^{aT} N_i^a)e + 2\varepsilon^{-1} \hat{v}^T N_i^{aT} N_i^a \hat{v} - 2e^T P \alpha_i \end{aligned} \tag{35}$$

According to the error dynamic, the two following cases can be investigated:

Case 1. First it is assumed that the estimation error is not zero, so $r = y - \hat{y} \neq 0$, then the following can be written:

$$\begin{aligned} &2\varepsilon^{-1} \hat{v}^T N_i^{aT} N_i^a \hat{v} - 2e^T P \alpha_i = 0 \\ &\alpha_i = \varepsilon^{-1} \hat{v}^T N_i^{aT} N_i^a \hat{v} P^{-1} C^T \frac{s}{\|s + \delta\|^2} \end{aligned} \tag{36}$$

where δ is a small positive scalar with a value ranging between 0 to 1, often referred to as tuning parameter which is used to reduce the chattering. Hence, the inequality presented in Eq. (35) will be:

$$\dot{V} \leq \sum_{i=1}^{M} (e^T ((A_i - L_i C)^T P + P(A_i - L_i C) + (\varepsilon e^T \mathrm{PM}_i^a M_i^{aT} P + 2\varepsilon^{-1} N_i^{aT} N_i^a)e \tag{37}$$

Case 2. In the second case, it is assumed that the estimation error is zero, therefore, $r = y - \hat{y} = 0$, then $\alpha_i = 0$:

$$\dot{V} = \sum_{i=1}^{M} (e^T ((A_i - L_i C)^T P + P(A_i - L_i C) + \varepsilon e^T P M_i^a M_i^{aT} P + 2\varepsilon^{-1} N_i^{aT} N_i^a)e \tag{38}$$

Hence, it can be concluded that the system converges asymptotically to zero if and only if:

$$(A_i - L_i C)^T P + P(A_i - L_i C) + \varepsilon e^T \mathrm{PM}_i^a M_i^{aT} P + 2\varepsilon^{-1} N_i^{aT} N_i^a < 0 \tag{39}$$

With the assumption of $W_i = PL_i$, Eq. (39) can be written as:

$$A_i^T P + PA_i - C^T W_i^T - W_i^T C + \varepsilon e^T P M_i^a M_i^{aT} P + 2\varepsilon^{-1} N_i^{aT} N_i^a < 0 \tag{40}$$

Using Lemma 2, the inequality in Eq. (40) can be written in the LMI form as follows:

$$\begin{bmatrix} A_i^T P + PA_i - C^T W_i^T - W_i^T C + \varepsilon N_i^a N_i^{aT} & PM_i^a \\ M_i^{aT} P & -\varepsilon^{-1} I \end{bmatrix} < 0 \tag{41}$$

Based on Theorem 1, by defining the P and W_i, the developed observer gain will be obtained from Eq. (42):

$$L_i = P^{-1} W_i \tag{42}$$

Sliding Mode gain for both Case 1 and 2 can be determined using the following expression:

$$\begin{cases} \text{If } r \neq 0 \quad \text{then } \alpha_i = \varepsilon^{-1} \hat{v}^T N_i^{aT} N_i^a \hat{v} P^{-1} C^T \frac{s}{\|s+\delta\|^2} \\ \text{If } r \neq 0 \quad \text{then } \alpha_i = 0 \end{cases} \tag{43}$$

Following the previous assumption for Case 2, Eq. (28), and $CC^T = I_P$, the value of Q can be obtained from the value of P, as follows:

$$P = C^T Q C$$
$$CQC^T = CC^T QCC^T$$
$$Q = CPC^T. \tag{44}$$

Consequently, taking into account that $V = S^T Q S > 0$, where $Q^T = Q > 0$, then $\dot{V} < 0$ is obtained, which means that the estimation error converges asymptotically to zero. Asymptotic convergence of estimation error guarantees the robustness of the proposed observers. To show the effectiveness of the proposed observers and prove their ability for state estimation, the Sliding Mode Observers developed in this study are implemented for multi-phase flow estimation case study of a large-scale process unit, using dynamic simulation model with numerical analysis.

3. Case study

Feasibility and effectiveness of the proposed observers developed in §2, are examined through a numerical simulation and real-life case study of multi-phase flow system. Multi-phase fluid flows can cause intense damage to pipelines, flow measurement instruments and specifically rotary equipment. Hence, all efforts are made to avoid or control the presence of multi-phase flow in designing the industrial processes. On the other hand, due to the nature of process systems, most of the time, presence of multi-phase flows in the process lines (e.g., steam-water utilities, power generation units, production units, etc.) is inevitable. In most process units where there is multi-phase fluid flow, there must be two separate subsystems for each phase to perform the process, and these two subsystems must necessarily be interconnected.

In this study a large-scale process system with several subsystems and two-phase flow input is considered for the case study. Liquid and gas units are the main subsystems of several interconnected subsystems within the plant. These two subsystems are interconnected, which means during the process, in the gas subsystem, some liquid is extracted that have to be sent to the liquid subsystem and in a similar way in the liquid subsystem, some gas is produced that must be sent to the gas subsystem. Fig. 2 illustrates a schematic of the multi-phase flow processes considered for the case study, where the flow enters the process unit in the form of two-phase composed of two large interconnected sub-systems. The processing unit for each flow phase is considered as the main sub-systems of the process unit. The sub-systems, their boundaries, inlets, and outlet conditions that are considered for the case study is described by Fig. 2.

In the system outlined in Fig. 2, in order to perform first stage (initial) separation, the multi-phase flow passes through a slug catcher as the first process unit. Given that the complete separation of the two phases cannot be achieved, the slug catcher includes two two-phase outlets, the first is a condensate line containing some gas and the second is a gas line which contains some condensate. The overall system is assumed to be decentralized system including two distinct but correlated sub-systems.

The sliding mode observer (SMO) design outlined in §2 is adopted to investigate the appropriateness and robustness of the proposed model for multi-phase flow measurement using numerical simulations and real-life case study data. Drift-flux model (DFM) is developed with the governing equations consisted of conservation of mass and momentum balance [38, 39, 50, 51]:

$$\frac{\partial(\rho\alpha)}{\partial t} + \frac{\partial(\rho\alpha u)}{\partial s} = \Phi + m \tag{45}$$

$$\frac{\partial(\rho\alpha u)}{\partial t} + \frac{\partial(\rho\alpha u^2)}{\partial s} = -\alpha\frac{\partial P}{\partial s} + \tau_w \frac{S}{A} + \varphi + \rho g \alpha \sin\theta \tag{46}$$

where ρ is the fluid density, P is the pipe line pressure, α denotes the volume fraction of each phase, u, t and s represent the velocity, time and spatial length in the pipeline, respectively. τ_w is the shear stress between surfaces, φ is the interfacial interaction, S denotes the effective wetted cross-section, A is the pipeline cross-section, θ is the pipe inclination angle, m is the mass transformation rate and Φ denotes the mass flow rate from external source. The numerical model is developed with the assumption of mass transfer between the phases is zero and the mass flow from external sources is equal to the interconnection flow between the subsystems.

By writing Eq. (45) and Eq. (46) for each subsystem separately, considering the interconnection between them, the law of conservation of mass can be written for liquid and gas individually and the conservation of momentum can be derived for the liquid and gas mixture. The description of the dynamic model employed in this study for conducting multi-phase flow simulations, and the detailed procedures steps to derive the governing equations, and discretization process can be found in [52]. Thus, the aggregated dynamic model of the distributed multi-phase flow system can be written as:

$$\frac{\partial v_i}{\partial t} = -\tilde{A}_i \frac{\partial v_i}{\partial s} + \tilde{Q}_i + \tilde{h}_j, \quad i \neq j = G, L$$
$$v = (P_g \; u_g \; \alpha_l)^T \tag{47}$$

where v is the state variable and P_g, u_g and α_l are gas phase pressure, gas phase velocity and liquid phase volume fraction, respectively. In Eq. (47), matrix A_i can be used instead of $\tilde{A}_i$, to simplify the notes:

$$v_t^i(s.t) = -A_i v_s^i(s,t) + Q_i(s,t) + h_j(s,t), \quad i,j = G, \; L \& i \neq j \tag{48}$$

$$y = \int_0^L C v(s,t) ds \tag{49}$$

The initial conditions are defined as follows:

$$v(0,t) = 0, \qquad v(L,t) = v_L \quad t \in [0,\infty]$$
$$v(s,0) = v_0(s) \quad s \in [0,L] \in R \tag{50}$$

By combining the equations of the two sub-systems as a matrix block, it can be written:

$$V_t(s,t) = -AV_s(s,t) + Q(s,t) + H(s,t) \tag{51}$$

It is evident that Eq. (51) is in the same form as Eq. (1), proving that the proposed observers are suitable for distributed multi-phase flow system and can be applied to its dynamic model described by Eq. (51).

4. Simulation results

The multi-phase flow measurements and the real data employed in this study were collected from a power plant process unit located in Iran. The numerical simulations were carried out using MATLAB and HYSYS in parallel. Table 1 summarizes the key parameters and boundary conditions of the real process measured for the subsystems.

Table 2 describes the 24-hrs averaged measured data for the real-life case study used for examining the performance of the proposed SMOs... The simulation of the system dynamics and the proposed SMOU and SMOD were carried out and the numerical results were validated based on the averaged real process data summarized in Table 2. The values presented in Table 2 are obtained based on the

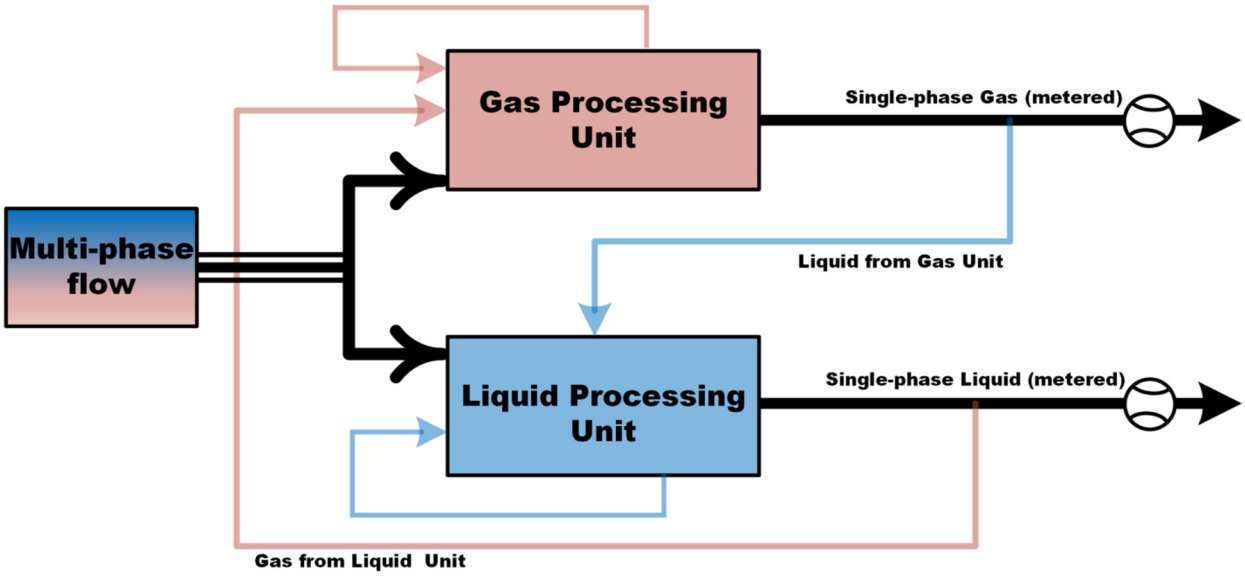

Fig. 2. Schematic of subsystems boundaries, inlets, and outlets for the case study process plant.

Table 1. Measured process parameters for the case study subsystems.

Parameter	Value	Unit
Inlet Pressure (P_I)	40	Bar
Inlet Pipe Diameter	0.609	M
Temperature (T)	35	Celsius
Gas Density (ρ_g)	98	Kg/m^3
Liquid Density (ρ_l)	750	Kg/m^3
Gas Pipe Diameter (D_g)	0.304	M
Liquid Pipe Diameter (D_l)	0.406	M

Table 2. 24-hr averaged measured input-output balance data for the case study process plant.

Products	Values (MMCMD)
Received Gas (By Downstream)	1.51
Sent Gas (By Upstream)	1.66
Condensate	0.06
Measured dry gas	1.34
Flare	0.003
Utility	0.06
Acid Gas	0.02
Water content	0.006

built design information of the process plant considered for the case study.

Fluctuations in the multi-phase flow parameters including flow, pressure, and temperature, are inevitable due to the inherent nature of the process described by the case study. To compensate for these fluctuations in the flow parameters, this study implements an auto-tuning feature to control the changes in flow and process parameters. The proportional and integral control (PI) parameters are used for tuning the controllers. Following the implementation of the auto-tuning feature, the proposed dynamic simulation model (described in §3) is capable of capturing input flow fluctuations and alter the output accordingly, by considering the effects of the changes in input conditions.

In practice, the input gas (two-phase gas from the upstream) is determined by measuring the single-phase gas as a metered gas and multiplying it by a shrinkage factor. The shrinkage factor is usually determined by the process designer and when the plant is first established. On the other hand, rich gas in the upstream is measured by an inaccurate single-phase flow meters such as venturi, orifice, or other differential pressure flow meters. According to Table 2, the measured dry gas for the case study investigated here is approximately 1.34 million m^3/day. Considering the process plant shrinkage factor of 1.13, the volume of received gas from the upstream operation unit will be 1.51 million m^3/day. The multi-phase flow characteristics described for the upstream of the case study plant, was measured by a differential pressure (DP) flow meter which provides a relatively inaccurate estimation of the flow. The sent upstream gas was measured as 1.66 million m^3 per day (Table 2). The flow measurement method used in the case study process unit is associated with a high degree of uncertainty, random and systematic error sources which has led to measurement error of approximately 9%. The measurement error is largely affected by the fluctuations in the volume of the mixture in the pipe, including the composition percentage of different flow phases, consumed fuel (gas or liquid fuel), gas-to-flare, and so forth, whereas the flow measurement system considers these parameters to be temporally constant. The shrinkage factor is also not a robust measure to adjust the multi-phase flow meter readings as it is derived based on the parameters that were measured when the plant was first established and does not reflect the temporal variations of these parameters. For the case study described here, the low precision of the upstream choke valve adjustment, inaccuracy of the single phase differential pressure flow meters, and the multi-phase nature of the flow at the outlet of upstream operation unit and the inlet of the plant also played key role in the estimation error of the multi-phase flow. Further, the performance and the efficiency of the flowmeters is usually assumed to be constant, despite the performance deterioration over the time.

The temporal variation of the gas and liquid-phase velocity in their subsystems are obtained from the HYSYS numerical simulation results and presented in Figs. 3 and 4, respectively. The numerical simulation results for each subsystem are compared with the Sliding Mode Observers (SMOU and SMOD) developed in this study (Figs. 3 and 4). P_0 and L_i matrices are determined for the case study by solving the inequality described in Eq. (41) for the multi-phase flow model using advanced optimization technique and the YALMIP solver in MATLAB, with the real process data described in Tables 1 and 2:

$$Po = \begin{bmatrix} 1.4650 & 1.5336 & 1.5583 \\ 1.5336 & 983.5776 & 42.7016 \\ 1.5583 & 42.7016 & 4.8770 \end{bmatrix}$$

$$L_1 = \begin{bmatrix} 170.1046 \\ 0.3922 \\ -9.6443 \end{bmatrix}$$

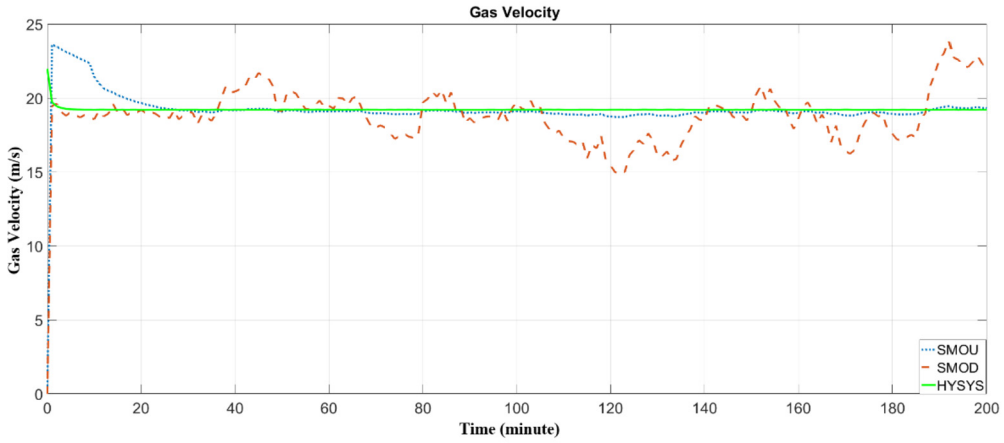

Fig. 3. Comparison of gas-phase velocity in the gas subsystem between HYSYS simulation, and the proposed SMOU and SMOD.

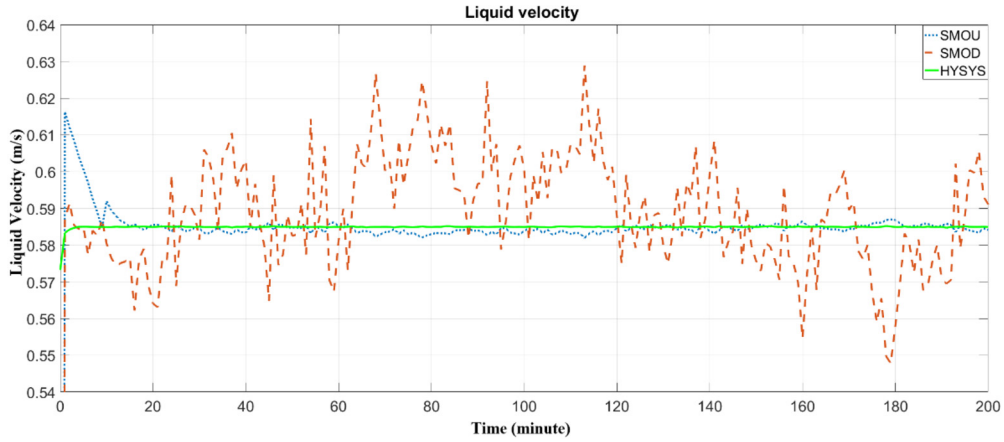

Fig. 4. Comparison of liquid-phase velocity in the liquid subsystem between HYSYS simulation, and the proposed SMOU and SMOD.

$$L_2 = \begin{bmatrix} 172.2728 \\ 1.3000 \\ -28.1502 \end{bmatrix}$$

The analysis of the simulation results shows that using the proposed Sliding Mode Observers, the estimation of all state variables converges to real measured values and the estimation error converges to zero (see Figs. 3–8), demonstrating the robust performance of the proposed observers. However, comparison of the proposed SMOs with the HYSYS simulations indicates that SMOU, i.e. interconnection is considered as uncertainty, has a higher accuracy and efficiency compared to the SMOD scenario, where the interconnection between sub-systems is considered as a disturbance.

Although the sliding mode terms have been added to certify the robustness against the uncertainty and disturbance in the process system, for the case of SMOU an overshoot is observed for the estimation of gas and liquid-phase velocities (Figs. 3 and 4, respectively). However, this overshoot is dampened rapidly with a relatively small settling time of approximately less than 10 secs, which indicates the appropriate performance of the designed observer. Further, analysis of the results shows that the estimation accuracy for the SMOU scenario is higher than SMOD, highlighting that the proposed SMO approach is well capable of capturing uncertainties in the multi-phase flow processes. Statistical analyses were conducted to examine the performance of the proposed Sliding Mode Observers. The results obtained from RMSE analysis confirm the robustness of SMOU for multi-phase flow estimations and admissible convergence rate.

Figs. 5 and 6 show the spatial variation of liquid and gas-phase velocities across the length of the pipe, respectively. The simulation data from HYSYS numerical model are compared with SMOD and SMOU estimations for the spatial variation of flow variables across the length of the pipeline. It is noticeable that fluid velocity decreases along the length of the pipeline for both liquid and gas phases, and the liquid-phase fraction increases due to the frictional pressure loss. The results presented in Figs. 5 and 6 show that although both SMOD and SMOU velocity estimations closely follow the simulation data, SMOU method shows higher estimation accuracy, when compared to the HYSYS simulations.

The temporal variations of the volume fraction in both liquid and gas subsystems are investigated. The volume fraction estimated by both proposed observers are compared with the real plant data simulation (Figs. 7 and 8). The overall analysis of the results shows that both observers can reasonably replicate the simulation data and estimate the multi-phase flow state variables. However, the estimation results for the observer that considers the interconnections of the subsystems as an uncertainty is more efficient and robust, compared to the observer that considers the interconnections of the subsystems as disturbance. The main reason that the proposed observer is more robust for the uncertainty (i.e. SMOU) than the disturbance (i.e. SMOD) is that, for the case study investigated here, the type of uncertainty that affects the interconnection of the subsystems is directly influence the system state variables, while disturbance indirectly affects both the state variables and parameters.

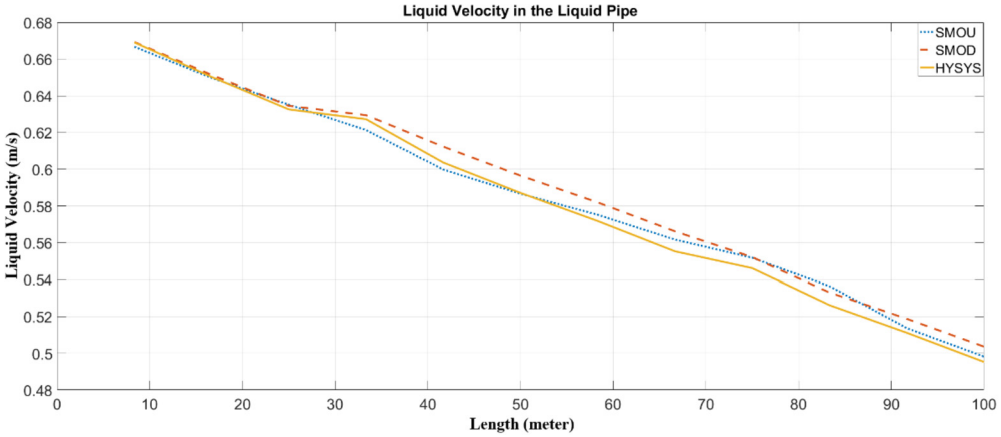

Fig. 5. Liquid velocity versus pipe length in the Liquid Pipe.

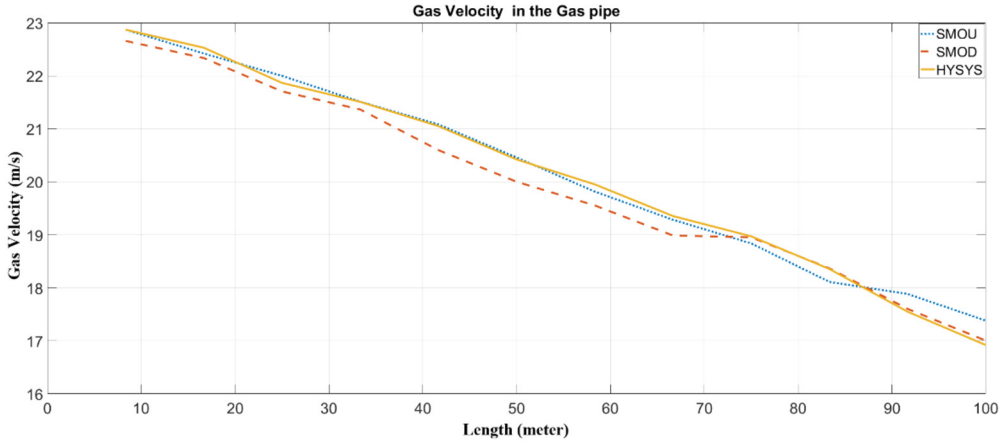

Fig. 6. Gas velocity versus pipe length in the Gas Pipe.

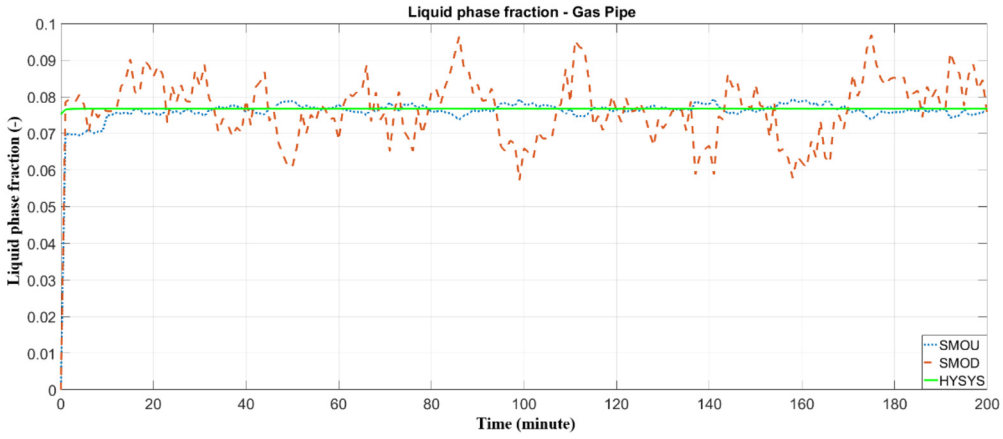

Fig. 7. Liquid phase fraction in the Gas Pipe.

Comparison of the results between HYSYS simulations and SMO estimations for the liquid phase fraction (Figs. 7 and 8) show an improved performance for both SMOD and SMOU, without the overshooting behavior that was observed for the gas and liquid-phase velocity estimation (i.e. Figs. 3 and 4). This difference in the estimation performance of the proposed SMOs is due to the fact that the phase velocity of the flow and the volume fraction of the phases have different effects on the equations that govern observers.

The measurement errors influencing the estimation results can be divided into two categories including the disturbances associated with the measurements, i.e. pressure signals and inlet/outlet multi-phase flow measurements (i.e. SMOD), and the uncertainties introduced to the system due to the variations in interconnection flows between the subsystems (i.e. SMOU). The statistical analysis of the results indicates that the estimation error of the states and variables are asymptotically stable and confirm robust performance of the proposed ob-

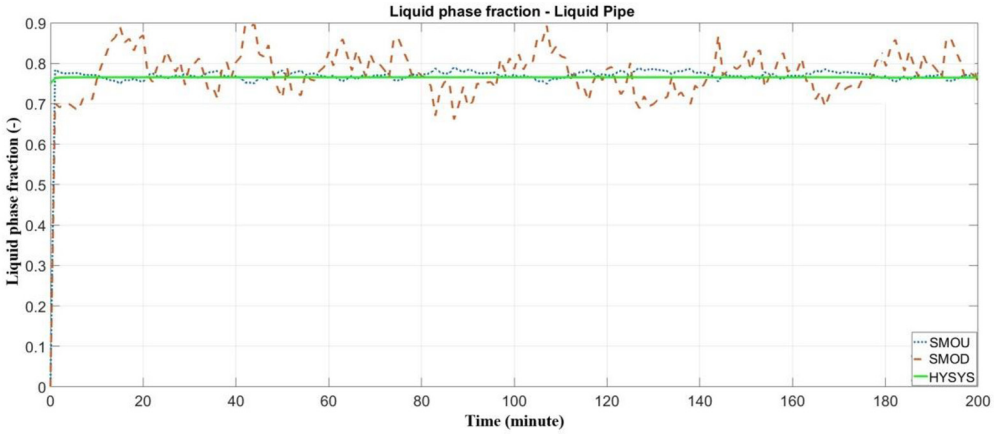

Fig. 8. Liquid phase fraction in the Liquid Pipe.

Table 3. RMSE metric for the state estimation by SMOU and SMOD.

Method	Parameters and variables			
	Gas velocity	Liquid velocity	Gas phase fraction	Liquid phase fraction
SMOU	$1 \cdot 8 \times 10^{-3}$	$2 \cdot 2 \times 10^{-3}$	$1 \cdot 2 \times 10^{-3}$	$1 \cdot 6 \times 10^{-3}$
SMOD	$2 \cdot \cdot 1 \times 10^{-3}$	$2 \cdot 6 \times 10^{-3}$	$4 \cdot 1 \times 10^{-3}$	$3 \cdot 3 \times 10^{-3}$

servers in estimating multi-phase flow measurement. Table 3 summarizes the RMSE values determined for the multi-phase flow estimations proposed by the SMOU and SMOD observers. The error analysis was conducted for both liquid and gas-phase velocity and phase fraction.

Comparison of the results obtained from the numerical simulation of the decentralized system described in §3 using dynamic HYSYS simulation with real data as a benchmark, with the proposed Sliding Mode Observers show that SMOU estimation of multi-phase flow parameters and variables is more aligned with the benchmark data compared to SMOD. The statistical analysis of the results (see Table 3) further confirms that the proposed SMOU outperforms the SMOD with respect to the estimation of the multi-phase velocities (i.e. gas and liquid-phase velocities), and phase fractions. The RMSE determined for both SMOD and SMOU show that the overall uncertainty which is introduced in the velocity and phase fraction estimation by SMOU observer is 0.24%, and for the case of SMOD this uncertainty is 0.46%. This highlight that although both observers are relatively capable of robust approximation of the states of multi-phase flow, SMOU observer has a superior performance. Given that precision of pressure measurement has a direct effect on the multi-phase flow variables and the variables' estimation in the subsystems, even small inaccuracy, or disturbance in the pressure recording will result in a significant error in the estimation of multi-phase velocities and phase fractions. Since at low flowrates the effects and significance of estimation error increases, the liquid subsystem variables show more significant error compared to the gas subsystem. Although the results show that all the states are estimated with admissible accuracy by both Sliding Mode estimators, the SMOU has better performance compared to the SMOD, based on the uncertainty analysis, and chattering reduction. However, the difference in estimation of the multi-phase flow characteristics between SMOU and SMOD is not significant. The simulation results demonstrate the high efficiency of both SMOU and SMOD scenarios without requiring high observer gain, suggesting that the proposed Sliding Mode Observers are appropriate and highly reliable for stable operational conditions. The average CPU time required to estimate the states using the SMOU and SMOD are 6.4 s and 7.2 s, respectively, which indicate that the computational algorithm developed within this study is acceptable from the computational efficiency point of view. A comparison of the two SMO scenarios shows that the two methods are not significantly different in terms of computational costs (i.e. CPU time).

5. Conclusion

Robust estimation of multi-phase flow characteristics is vital for the design and operation of a wide range of environmental and industrial processes. However, accurate multi-phase flow measurement is a difficult task due to the nonlinear and spatiotemporally varying nature of the multi-phase fluid flows. This study develops Sliding Mode Observers for decentralized estimation of multi-phase flow parameters. The performance of the proposed observers is evaluated for two scenarios, where first the interconnections between two multi-phase subsystems are considered as a disturbance, and the second scenario considers the interconnections between the subsystems as an uncertainty.

Drift Flux Model (DFM) is developed to simulate multi-phase fluid flow for a case study considering multi-phase flow of gas-liquid in a process plant system. The plant's main units are considered as subsystems of an overall decentralized system. DFM equations are converted into conventional equations, to design the decentralized nonlinear observer considering the complex interconnections between the subsystems. Performance of the developed sliding mode observers, i.e. SMOU and SMOD, is then examined for estimating the input multi-phase flow for the case study data. Given that the general system can be considered as two interconnected subsystems including condensate and gas, the interconnections between the two subsystems are investigated as a disturbance and uncertainties, respectively. The stability of the error between SMO estimations and the real-life case study variables are proved based on the Lyapunov method. All the numerical simulations were conducted based on the measured information obtained from a real multi-phase flow process, and the performance of the observer's estimation is evaluated with use of the real data. Analysis of the results show that all the states and variables are estimated with good precision by both proposed SMOU and SMOD observers. The statistical analysis of the results and comparison to the measured data highlights that the SMOU provides more robust performance in estimating multi-phase flow characteristics compared to the SMOD. The simulation results indicate the high efficiency of both SMOU and SMOD in estimation of multi-phase flow

variables with no need for a high observer gain, confirming the appropriateness and robustness of the proposed Sliding Mode Observers for multi-phase flow measurements in stable operational conditions.

Nomenclature:

Symbol	Description
p_g	Gas Pressure (bar)
p_l	Liquid Pressure (bar)
ρ_g	Gas Density (kg/m^3)
ρ_l	Liquid Density (kg/m^3)
α_l	Liquid volume fraction (–)
α_g	Gas volume fraction (–)
u_g	Gas velocity (m/s)
u_l	Liquid velocity (m/s)
Φ	External source mass flow (kg/hr.)
h_G	Gas from liquid subsystem (kg/hr.)
h_L	Liquid from gas subsystem (kg/hr.)
T	Time (s)
$[\ ]_{Liquid}$	Equation of Liquid subsystem
φ	interfacial interaction (kg/m^2 s^2)
S_{fri}	friction losses (kg/m^2 s^2)
θ	pipe inclination angle (degree)
A	Pipe's Cross section (m^2)
M	Mass transfer (kg/hr.)
G	Gravitational constant (m/s^2)
τ_w	Shear stress between surfaces (N/m^2)
Q_i	Overall source term
H_i	Overall interconnection term
F_i	Flux
U_i	State variable vector
S	Space (m)
$[\ ]_{Gas}$	Equation of Gas subsystem
LMI	Linear Matrix Inequality

Declarations

Author contribution statement

Abolfazl Varvani Farahani & Soroush Abolfathi: Conceived and designed the experiments; Performed the experiments; Analyzed and interpreted the data; Contributed reagents, materials, analysis tools or data; Wrote the paper.

Funding statement

This research did not receive any specific grant from funding agencies in the public, commercial, or not-for-profit sectors.

Data availability statement

Data will be made available on request.

Declaration of interests statement

The authors declare no conflict of interest.

Additional information

No additional information is available for this paper.

References

[1] N. Ayuba, R.D.B. Buhler, L. Silva, T.J. Lopes, Application of density – viscosity in predicting oil – water flow profile in horizontal pipe, Exp. Comput. Multiph. Flow 4 (2022) 52–70.

[2] S. Borzooei, R. Teegavarapu, S. Abolfathi, Y. Amerlinck, I. Nopens, M.C. Zanetti, Impact evaluation of wet-weather events on influent flow and loadings of a water resource recovery facility, in: International Conference on Urban Drainage Modelling, 2018, pp. 706–711.

[3] S. Borzooei, G.H. Miranda, S. Abolfathi, G. Scibilia, L. Meucci, M.C. Zanetti, Application of unsupervised learning and process simulation for energy optimization of a WWTP under various weather conditions, Water Sci. Technol. 81 (8) (2020) 1541–1551.

[4] S. Borzooei, A. Youri, D. Panepinto, S. Abolfathi, N. Ingmar, S. Gerardo, M. Lorenza, M.C. Zanetti, Energy optimization of a wastewater treatment plant based on energy audit data: small investment with high return, Environ. Sci. Pollut. Res. (2020) 1–14.

[5] Y. Li, M. Hosseini, H. Arasteh, D. Toghraie, S. Rostami, Transition simulation of two-phase intermittent slug fl ow characteristics in oil and gas pipelines, Int. Commun. Heat Mass Transf. 113 (2020) 104534.

[6] B.Y. Kaplan, A.A. Motorin, E.L. Stupitsky, Research of a two-phase steam system during its flow in the pipe and a device for measuring dryness steam, Mater. Sci. Eng. 927 (1) (2020) P.012072.

[7] R.C. Baker, Flow Measurement Handbook, 2000.

[8] M. Leskens, J.P.M. Smeulers, A. Gryzlov, Downhole Multiphase Metering in Wells by Means of Soft-Sensing, 2008.

[9] M. Najmedini, R. Habibi, Multiphase flow meter: a review, in: Oil, Gas Petrochemicals Lett., vol. 2, 2017, pp. 1–13.

[10] J. Luiz, G. Oliveira, J. César, R. Verschaeren, C. Van Der Geld, Mass flow rate measurements in gas – liquid flows by means of a venturi or orifice plate coupled to a void fraction sensor, Exp. Therm. Fluid Sci. 33 (2) (2009) 253–260.

[11] D.L. Gysling, E. Meters, Clamp-on two phase measurement of gas condensate wells using integrated equation of state compositional models, in: 28th International North Sea Flow Measurement Workshop, 2010, pp. 1–18.

[12] Y.M. Xuewei Shia ChaoTanb, Feng Donga, Oil-gas-water three-phase flow characterization and velocity measurement based on time-frequency decomposition, Int. J. Multiph. Flow 111 (2019) 219–231.

[13] K. Sarkodie, A. Fergusson-rees, P. Diaz, A review of the application of non-intrusive infrared sensing for gas – liquid flow characterization, J. Comput. Multiph. Flows 10 (1) (2018) 43–56.

[14] Y.D. Baba, A.M. Aliyu, A. Archibong, Study of high viscous multiphase phase flow in a horizontal pipe, Heat Mass Transf. 54 (2017) 1–19.

[15] C. Tan, J. Jia, C. Xu, Z. Sun, F. Ding, Multiphase flow measurement: techniques and applications, IEEE Access 6 (2018) 32673–32675.

[16] M.H. Silva, E. Chacon, I.T. Garcia, D.A. Rosendahl, M. Teixeira, R.S. Farias, Metrological concerns in multiphase flow measurement, J. Phys. 1044 (1) (2018) 012046.

[17] A.H.W.Y. Sun, W. Bao, K. Valk, C.C. Brauer, J. Sumihar, Improving forecast skill of lowland hydrological models using ensemble Kalman filter and unscented Kalman filter water resources research, Water Resour. Res. 56 (8) (2020) E2020WR027468.

[18] G. Cerati, P. Elmer, P. Aditya, E. Apriliani, D. Khusnul, Estimation of water level and steam temperature using ensemble Kalman filter square root (EnKF-SR), J. Phys. Conf. Ser. 1008 (1) (2018) 012026.

[19] M. Elshafei, M.A. Habib, Softsensor for estimation of steam quality in riser tubes of boilers, J. Mech. Eng. Sci. 227 (10) (2012) 2337–2347.

[20] E.N.D.O.S. Santos, et al., Sensing platform for two-phase flow studies, IET Sci. Meas. Technol. 7 (2019) 5374–5382.

[21] Y. Yan, L. Wang, T. Wang, X. Wang, Y. Hu, Q. Duan, Application of soft computing techniques to multiphase fl ow measurement: a review, Flow Meas. Instrum. 60 (March 2018) 30–43.

[22] H. Dimassi, J.J. Winkin, A. Vande, A sliding mode observer for a linear reaction – convection – diffusion equation with disturbances, Syst. Control Lett. 124 (2019) 40–48.

[23] W. Yan, J. Fei, Adaptive control of MEMS gyroscope based on global terminal sliding mode controller, Mathematical Problems in Engineering 2013 (2013).

[24] H. Ríos, et al., An adaptive sliding-mode observer for a class of uncertain nonlinear systems, Int. J. Adapt. Control Signal Process. 32 (3) (2018) 511–527.

[25] T. Ristanto, Machine Learning Applied to Multiphase Production Problems, Master's thesis, Stanford University, Stanford, California, USA, 2018.

[26] R. Cui, L. Chen, C. Yang, S. Member, Extended state observer-based integral sliding mode control for an underwater robot with unknown disturbances and uncertain nonlinearities, IEEE Trans. Ind. Electron. 64 (8) (2017) 6785–6795.

[27] V. Van Huynh, B. Le, N. Minh, E.N. Amaefule, A. Tran, Highly robust observer SlidingMode based frequency control for multi area power systems with renewable power plants, Electronics 10 (3) (2021) 274.

[28] A. Varvani Farahani, M. Montazeri, Multi-phase flow measurement in a gas refinery using decentralized Lyapunov – based adaptive observer, Trans. Inst. Meas. Control 43 (3) (2021) 700–716.

[29] H. Li, Y. Yang, Y. Wei, F. Dai, Observer-based fault reconstruction for linear systems using adaptive sliding mode method, J. Robot. Netw. Artif. Life 3 (4) (2017) 236–239.

[30] A. Nikoofard, T.A. Johansen, G.O. Kaasa, Reservoir characterization in underbalanced drilling using low-order lumped model, J. Process Control 62 (2018) 24–36.

[31] S.K. Kommuri, S.B. Lee, K.C. Veluvolu, Robust sensors-fault-tolerance with sliding mode estimation and control for PMSM drives, IEEE/ASME Trans. Mechatron. 23 (1) (2018) 17–28.

[32] H. Li, Y. Yang, Y. Wei, F. Dai, C. Systems, E. Science, Observer-based fault reconstruction for linear systems using adaptive sliding mode method, J. Robotics Netw. Artif. Life 3 (4) (2017) 236–239.
[33] H. Sedigh, M.A. Shoorehdeli, Fuzzy robust fault estimation scheme for a class of nonlinear systems based on an unknown input sliding mode observer, J. Vib. Control 13 (1) (2016).
[34] S.K. Kommuri, S. Bin Lee, Robust sensors-fault-tolerance with sliding mode estimation and control for PMSM drives, IEEE/ASME Trans. Mechatron. 23 (1) (2018) 17–28.
[35] J. Augusto, J. Cabas, S. Ph, D.M. Sanjúan, Liquid Transport Pipeline Monitoring Architecture Based on State Estimators for Leak Detection and Location, Master's thesis, Universidad del Norte, 2018.
[36] F. Piltan, J. Kim, Control of an uncertain robot manipulator using an observation-based modified fuzzy sliding mode controller, Int. J. Intell. Syst. Appl. 10 (3) (2018) 41.
[37] R. Galvan, L. Fridman, R. Iriarte, Integral sliding-mode observation and control for switched uncertain linear time invariant systems: a robustifying strategy, Asian J. Control 20 (4) (2018) 1551–1565.
[38] S. Mobayen, D. Baleanu, F. Tchier, Second-order fast terminal sliding mode control design based on LMI for a class of non-linear uncertain systems and its application to chaotic systems, J. Vib. Control 23 (18) (2017) 2912–2925.
[39] A.V. Farahani, M. Montazeri, Robust optimal decentralized observer for multi-phase flow measurement, Trans. Inst. Meas. Control 42 (4) (2020) 904–916.
[40] A.V. Farahani, M. Montazeri, Computational method for multiphase flow characterization in the gas refinery, Heliyon 6 (2020) e03193.
[41] M.M. Abolfazl. Varvani Farahani, Robust optimal decentralized observer for multi-phase flow measurement, Trans. Inst. Meas. Control 42 (4) (2020) 904–916.
[42] D. Goodarzi, S. Abolfathi, S. Borzooei, Modelling solute transport in water disinfection systems: effects of temperature gradient on the hydraulic and disinfection efficiency of serpentine chlorine contact tanks, J. Water Process Eng. 37 (2020) 101411.
[43] D. Goodarzi, K. Sookhak Lari, E. Khavasi, S. Abolfathi, Large eddy simulation of turbidity currents in a narrow channel with different obstacle configurations, Sci. Rep. 10 (2020) 12814.
[44] S. Borzooei, Y. Amerlinck, D. Panepinto, et al., Energy optimization of a wastewater treatment plant based on energy audit data: small investment with high return, Environ. Sci. Pollut. Res. 27 (2020) 17972–17985.
[45] A.V. Farahani, M. Montazeri, Computational method for multiphase flow characterization in the gas refinery, Heliyon 6 (2020) e03193.
[46] F.D. Bijnan Bandyopadhyay, K.-S. Kim, Sliding Mode Control Using Novel Sliding Surfaces, vol. 392, Springer, 2009.
[47] N. Kapoor, J. Ohri, Integrating a few actions for chattering reduction and error convergence in sliding mode controller in robotic manipulator, Int. J. Eng. Res. Technol. 2 (5) (2013) 466–472.
[48] V.B.S. Boyd, L.E. Ghaoui, E. Ferron, Linear Matrix Inequalities in Systems and Control Theory, Philadelphia: Studies in Applied Mathematics, SIAM, 1994.
[49] Fengxiang Chen, Weidong Zhang, LMI criteria for robust chaos synchronization of a class of chaotic systems, Nonlinear Anal. 67 (12) (2007) 3384–3393.
[50] O. Aarsnes, U.J.F. Di Meglio, F. Evje, S. Aamo, Control-Oriented Drift-Flux Modeling of Single and Two-Phase Ow for Drilling, 2014.
[51] R.F.M.A. Gryzlov, M. Leskens, A semi-implicit approach for fast parameter estimation by means of the extended Kalman filter, J. Process Control 21 (2011) 510–518.
[52] M.M. Abolfazl Varvani Farahani, Evaluation of Lyapunov-based observer using differential mean value theorem for multiphase flow characterization, SPE Prod. Oper. 35 (04) (2020) 0865.